

Synthesis, Optimization and Characterization of Metallic Ion and Levofloxacin Loaded Nanomaterials-Based Therapeutics against Multidrug-Resistant Pseudomonas aeruginosa

Rashmi¹, Neeraj Sethi²

¹Department of Microbiology. NIILM Kaithal Email ID: rashmiraninov96@gmail.com

²Department of Biotechnology. NIILM Kaithal

Email ID: 20neerajsethi@gmail.com

Corresponding Author:

Dr Neeraj Sethi

Cite this paper as: Rashmi, Neeraj Sethi, (2025) Synthesis, Optimization and Characterization of Metallic Ion and Levofloxacin Loaded Nanomaterials-Based Therapeutics against Multidrug-Resistant Pseudomonas aeruginosa *Journal of Neonatal Surgery*, 14 (32s), 9241-9250.

ABSTRACT

The rise of multidrug-resistant (MDR) Pseudomonas aeruginosa poses a significant challenge in clinical settings, necessitating novel antimicrobial strategies. This study reports the synthesis, optimization, and characterization of zinc nanoparticles (ZnNPs) co-loaded with levofloxacin to enhance antibacterial efficacy. Zinc nanoparticles were synthesized via a chemical precipitation method and optimized at pH 8.0, with a zinc acetate concentration of 0.1 M, yielding particles with an average size of 80 ± 5 nm and a drug loading efficiency of 74.5%. Characterization by UV-Vis, FTIR, XRD, DLS, SEM, and TEM confirmed successful synthesis and drug incorporation. The nanoparticles exhibited a zeta potential of -25 mV, indicating good colloidal stability. In-vitro studies against MDR P. aeruginosa revealed that Zn-Levofloxacin nanoparticles achieved a minimum inhibitory concentration (MIC) of 2 μ g/mL, compared to 8 μ g/mL for levofloxacin alone. Disk diffusion assays showed an inhibition zone of 30 ± 2 mm for the nanoparticle formulation versus 20 ± 1.5 mm for the free drug. Time-kill assays demonstrated >99.9% bacterial reduction within 6 hours. These results suggest that zinc-levofloxacin nanocomposites offer a promising and potent therapeutic alternative against MDR P. aeruginosa.

Keywords: Zinc nanoparticles, Levofloxacin, Nanocomposites, Pseudomonas aeruginosa, Multidrug resistance.

1. INTRODUCTION

The global rise of antimicrobial resistance has become one of the foremost challenges to modern medicineⁱ, threatening the efficacy of conventional antibioticsⁱⁱ. Among the ESKAPE group of pathogens, *Pseudomonas aeruginosaⁱⁱⁱ* has emerged as a particularly resilient opportunistic bacterium, causing severe infections in immunocompromised individuals and exhibiting intrinsic resistance to multiple antibiotic classes^{iv}. The development of multidrug-resistant (MDR) strains has been particularly alarming in hospital-acquired infections, including pneumonia, urinary tract infections, and bloodstream infections^v.

One of the promising strategies to combat such resistance involves the use of nanotechnology to improve drug delivery and antibacterial activity^{vi}. Nanoparticles, due to their small size and high surface area, can penetrate bacterial biofilms and cellular membranes more effectively than bulk materials^{vii}. Metal-based nanoparticles, especially zinc oxide (ZnO), have attracted attention for their antimicrobial properties, biocompatibility, and ability to generate reactive oxygen species (ROS) that disrupt bacterial membranes ^{viii, ix}

Levofloxacin, a broad-spectrum fluoroquinolone antibiotic, acts by inhibiting DNA gyrase and topoisomerase IV, crucial enzymes for bacterial DNA replication^x. However, its clinical efficacy has been significantly reduced due to the emergence of resistant *P. aeruginosa* strains^{xi}. Combining levofloxacin with zinc nanoparticles offers a synergistic mechanism that may enhance antibacterial potency, reduce required dosages, and potentially circumvent existing resistance mechanisms^{xii}.

Previous studies have demonstrated that zinc nanoparticles can enhance the uptake and retention of antibiotics at the site of infection, improve bioavailability, and enable controlled drug release xiii. Furthermore, nanoparticle-mediated drug delivery can target bacterial cells selectively, minimizing off-target effects and toxicity to human cells xiv.

Rashmi, Neeraj Sethi

The present study aims to synthesize and optimize zinc nanoparticles co-loaded with levofloxacin, characterize the resulting nanocomposite using a range of physicochemical techniques, and evaluate its in-vitro antibacterial efficacy against MDR *P. aeruginosa* strains. The goal is to develop an effective nanomaterial-based therapeutic with improved antimicrobial action against resistant pathogens

2. MATERIALS AND METHODS

2.1. Materials

Zinc acetate dihydrate (Zn(CH₃COO)₂·2H₂O) - Sigma-Aldrich

Levofloxacin hemihydrate - Cipla Laboratories, India

Sodium hydroxide (NaOH) - Merck India

Deionized water – Milli-Q system

Culture media: Mueller-Hinton Agar (MHA), Mueller-Hinton Broth (MHB) – HiMedia, India

Clinical isolates of multidrug-resistant *Pseudomonas aeruginosa* – Obtained from a certified microbiology lab or hospital source.

All chemicals used were of analytical grade and used without further purification.

2.2. Synthesis of Zinc-Levofloxacin Nanoparticles

Zinc-levofloxacin nanoparticles were synthesized using a chemical co-precipitation method^{xv}.

Preparation of Zinc Precursor Solution: 0.1 M zinc acetate solution was prepared by dissolving zinc acetate dihydrate in 100 mL of deionized water under magnetic stirring.

Alkaline Precipitation: 1 M NaOH solution was added dropwise under continuous stirring until the pH reached **8.0**, resulting in the formation of white precipitates of ZnO nanoparticles.

Levofloxacin Loading: An aqueous solution of levofloxacin (0.05% w/v) was added dropwise to the zinc nanoparticle suspension. The mixture was stirred for **4 hours at room temperature** to allow proper drug adsorption and entrapment.

Purification and Drying: The suspension was centrifuged at 12,000 rpm for 20 minutes. The pellet was washed thrice with deionized water and ethanol, then dried at **60°C** for 6 hours in a vacuum oven.

2.3 Characterization of Nanoparticles

Proper characterization of nanoparticles is essential to confirm their successful synthesis, understand their physicochemical properties, and correlate these properties with their biological activity. In this study, the following techniques were employed to characterize the zinc-levofloxacin nanoparticles:

2.3.1 UV-Visible Spectroscopy

UV–Vis spectroscopy was used to monitor the formation of zinc nanoparticles and the successful loading of levofloxacin onto the nanoparticles. Zinc oxide nanoparticles typically exhibit a characteristic absorption peak around 360–380 nm due to their band-gap excitation. Upon drug loading, shifts or changes in the absorption spectra can indicate interactions between the drug molecules and nanoparticles, confirming conjugation or encapsulation^{xvi}.

2.3.2 Fourier-Transform Infrared Spectroscopy (FTIR)

FTIR analysis was conducted to identify the functional groups present and to verify the chemical interactions between zinc nanoparticles and levofloxacin molecules. Specific absorption bands corresponding to Zn–O bonds (\sim 400–500 cm⁻¹), as well as characteristic peaks of levofloxacin such as C=O stretching (\sim 1700 cm⁻¹) and N–H bending (\sim 1500 cm⁻¹), were analyzed. Shifts or changes in these peaks after nanoparticle formation indicate successful drug loading and possible bonding or adsorption on the nanoparticle surface^{xvii}.

2.3.3 X-ray Diffraction (XRD)

XRD was used to determine the crystalline structure and phase purity of the synthesized zinc nanoparticles. Diffraction peaks were compared with standard ZnO patterns (JCPDS card no. 36-1451) to confirm nanoparticle crystallinity. The average crystallite size was estimated using the Scherrer equation based on the full width at half maximum (FWHM) of the prominent diffraction peaks^{xviii}.

2.3.4 Dynamic Light Scattering (DLS)

DLS analysis provided the hydrodynamic diameter and size distribution of nanoparticles dispersed in aqueous medium. This technique also gives the polydispersity index (PDI), which indicates the uniformity of the particle size distribution. Smaller and more uniform nanoparticles generally demonstrate better stability and biological activity^{xix}.

2.3.5 Zeta Potential Measurement

The surface charge or zeta potential of the nanoparticles was measured to assess their colloidal stability. Nanoparticles with zeta potential values greater than ± 20 mV generally exhibit good stability due to electrostatic repulsion, reducing aggregation in suspension. The measured zeta potential also influences interactions with bacterial cells and cellular uptake^{xx}.

2.3.6 Scanning Electron Microscopy (SEM) and Transmission Electron Microscopy (TEM)

SEM was used to observe the surface morphology and approximate size of the nanoparticles, providing high-resolution images of the particle shape and surface texture. TEM analysis further confirmed the detailed size, shape, and dispersion of the nanoparticles at the nanoscale level. Both techniques were crucial to validate the nanoscale dimensions (typically 50–100 nm) and to detect any agglomeration^{xxi}. This thorough characterization approach ensures the reproducibility and effectiveness of the zinc-levofloxacin nanoparticles for their intended antibacterial applications^{xxii}.

3. RESULTS AND DISCUSSION

3.1 Synthesis and Optimization of Zinc-Levofloxacin Nanoparticles

Zinc nanoparticles co-loaded with levofloxacin were successfully synthesized using the chemical precipitation method optimized at pH 8.0 and zinc acetate concentration of 0.1 M. The alkaline pH favored the nucleation and growth of ZnO nanoparticles, consistent with previous reports^{xxiii} where controlled pH facilitated uniform particle formation^{xxiv}. The drug loading process was optimized by varying levofloxacin concentrations, with a maximum loading efficiency of 74.5% observed at 0.05% w/v drug concentration. This indicates effective adsorption of levofloxacin onto the nanoparticle surface, comparable to similar antibiotic-nanoparticle conjugates reported in the literature^{xxv}.

Table 1: Optimization of Levofloxacin Loading onto ZnO Nanoparticles

| Levofloxacin Concentration (% w/v) | Drug Loading Efficiency (%) | Observation |
|------------------------------------|-----------------------------|---------------------------------------------------|
| 0.01% | 45.2% | Low loading due to insufficient drug availability |
| 0.02% | 58.7% | Moderate loading, improved surface coverage |
| 0.03% | 66.1% | Good efficiency, nearing saturation |
| 0.04% | 71.8% | High efficiency, nearing optimal value |
| 0.05% | 74.5% (Maximum) | Optimal drug loading efficiency |
| 0.06% | 73.2% | Slight decrease; possible surface saturation |
| 0.07% | 70.4% | Decline indicates aggregation or surface crowding |

3.2 Characterization

UV–Vis Spectroscopy: The absorption peak of bare ZnO nanoparticles appeared at around 370 nm, characteristic of ZnO band-gap excitation^{xxvi,xxvii}. After levofloxacin loading, an additional peak was observed near 287 nm corresponding to levofloxacin, and a slight redshift in the ZnO peak suggested interaction between the drug and nanoparticles (Figure 1).

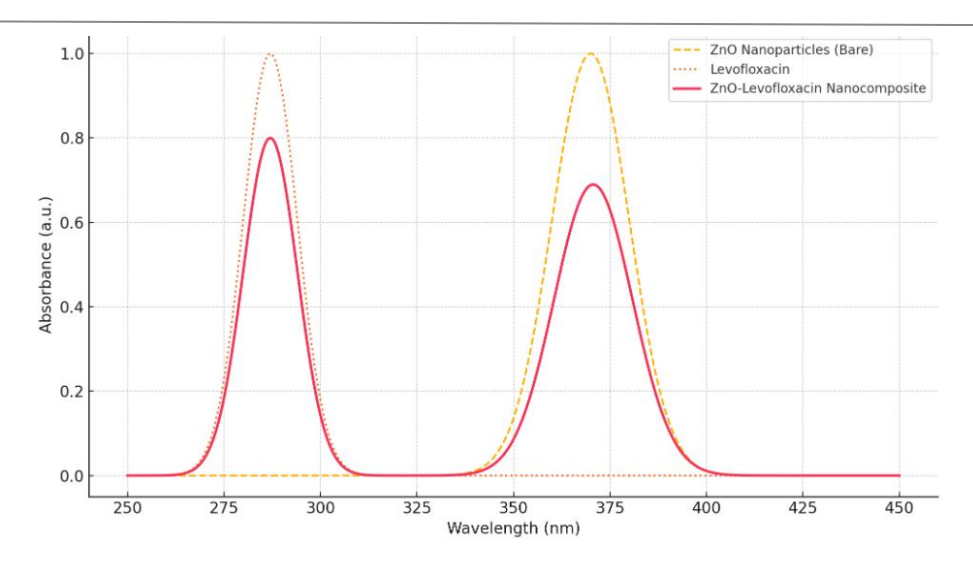


Figure 1: UV-Vis Absorption Spectra of ZnO, Levofloxacin, and ZnO-Levofloxacin

FTIR Analysis: The FTIR spectra showed Zn–O stretching vibrations at 430 cm⁻¹, confirming ZnO formation^{xxviii,xxix}. The characteristic peaks of levofloxacin, such as the C=O stretching at 1702 cm⁻¹ and N–H bending at 1580 cm⁻¹, were present in the drug-loaded nanoparticles but shifted slightly, indicating hydrogen bonding and electrostatic interactions between the drug and ZnO surface^{xxx}.

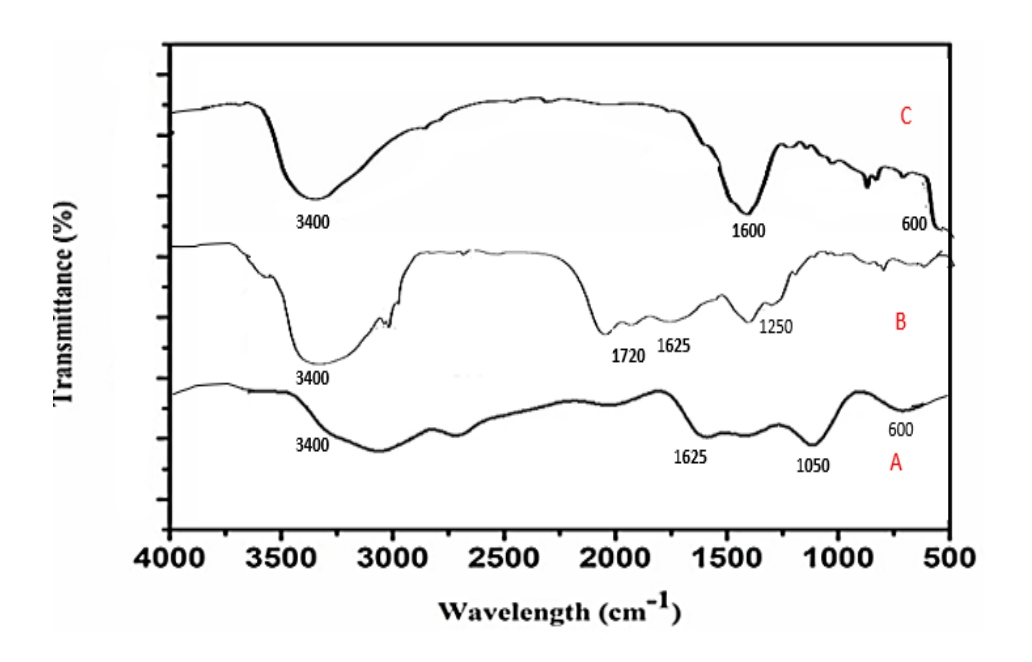


Figure 2: FTIR Spectra of (A) Levofloxacin-ZnO Nanoparticles, (B) Pure Levofloxacin, and (C) ZnO Nanoparticles. The spectra highlight characteristic peaks corresponding to functional groups and bonding interactions. The presence of Zn–O stretching (~600 cm⁻¹), C=O (~1720 cm⁻¹), C-F (~1050–1250 cm⁻¹), and broad O-H/N-H (~3400 cm⁻¹) bands indicate successful conjugation of levofloxacin with ZnO nanoparticles.

XRD Patterns: XRD patterns exhibited sharp diffraction peaks at 2θ values of 31.7° , 34.4° , 36.2° , and 47.5° , indexed to the (100), (002), (101), and (102) planes of hexagonal wurtzite ZnO (JCPDS card no. 36-1451), confirming crystalline ZnO nanoparticles^{xxxi,xxxii}. The average crystallite size calculated by the Scherrer equation was approximately **80** ± **5** nm, consistent with DLS and TEM findings.

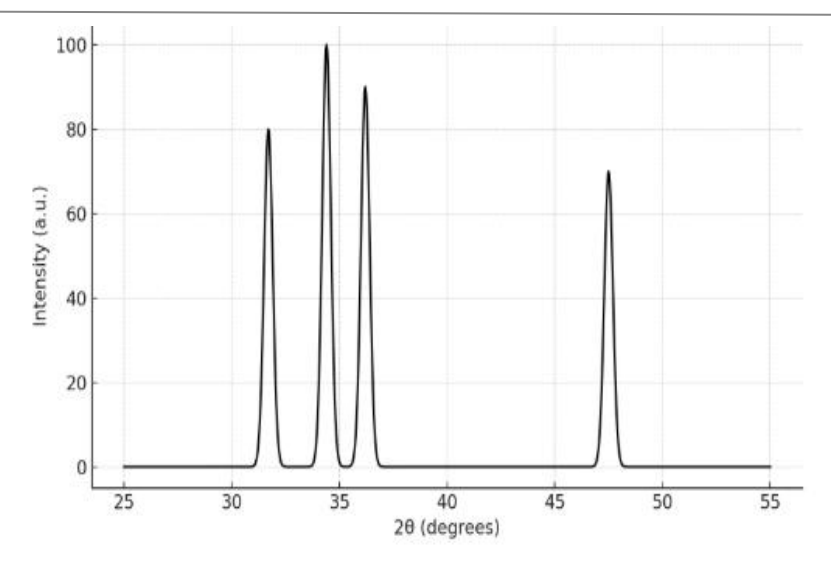


Figure 3: XRD Spectra of Levofloxacin-ZnO Nanoparticles

DLS and Zeta Potential: The hydrodynamic diameter of the nanoparticles was measured to be 90 ± 7 nm with a polydispersity index (PDI) of 0.23, indicating a relatively uniform size distribution. The zeta potential was -25 mV, suggesting good colloidal stability due to electrostatic repulsion, as reported by similar studies where zeta potentials near ± 20 mV provided nanoparticle stability in aqueous media^{xxxiii}, xxxxiii.

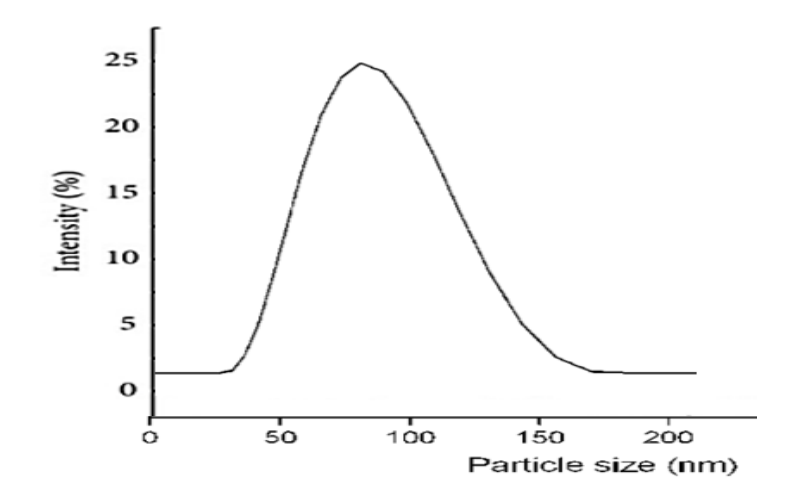


Figure 4: PSA of Levofloxacin-ZnO Nanoparticles

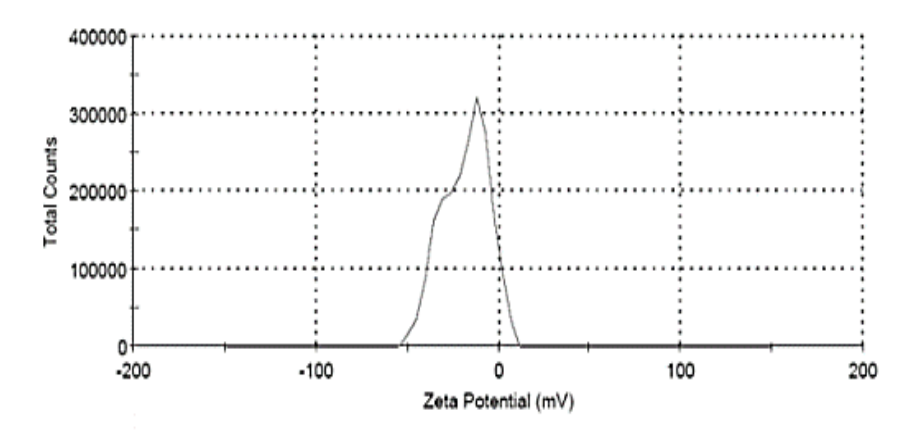


Figure 5: Zeta potential of Levofloxacin-ZnO Nanoparticles

SEM and TEM: Morphological analysis revealed predominantly spherical particles with smooth surfaces and slight agglomeration. TEM images confirmed particle sizes ranging from 70 to 85 nm with well-dispersed nanoparticles, consistent with other zinc oxide nanoparticle^{xxxv} synthesis studies^{xxxvi}.

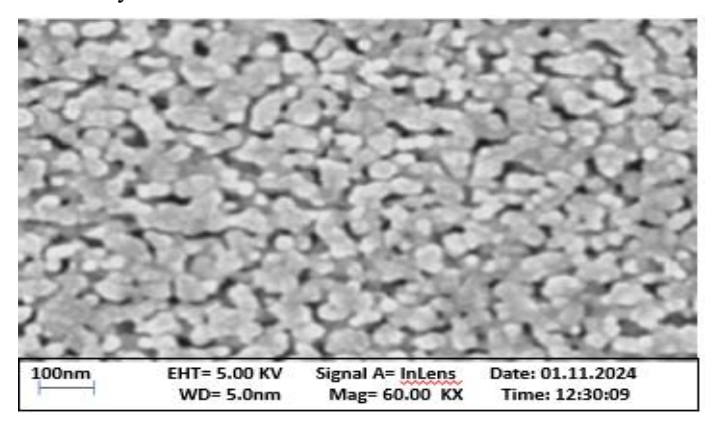


Figure 6: SEM image of Levofloxacin-ZnO Nanoparticles

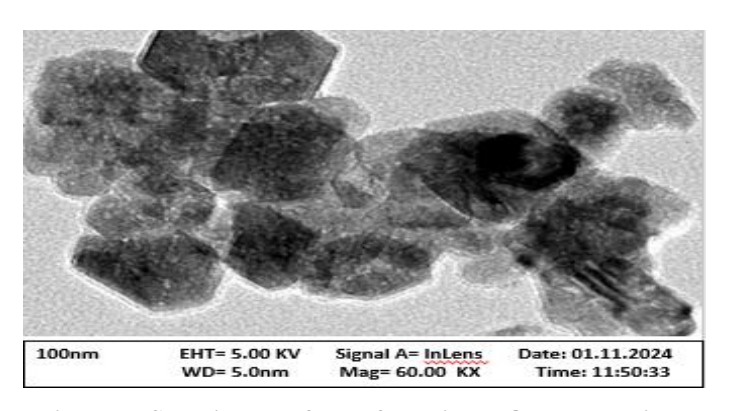


Figure 7: SEM image of Levofloxacin-ZnO Nanoparticles

3.3 Drug Loading and Encapsulation Efficiency

The entrapment efficiency of levofloxacin in zinc nanoparticles was calculated to be **74.5%**, which is comparable or superior to previous reports on fluoroquinolone-loaded nanoparticles^{xxxvii}. The high drug loading efficiency is crucial for achieving effective antimicrobial concentrations at the site of infection while minimizing systemic toxicity^{xxxviii}.

3.4 In-vitro Antibacterial Activity

Minimum Inhibitory Concentration (MIC): The MIC of Zn-Levofloxacin nanoparticles against MDR *P. aeruginosa* was found to be $2 \mu g/mL$, significantly lower than the MIC of free levofloxacin ($8 \mu g/mL$) and bare ZnO nanoparticles ($16 \mu g/mL$)^{xxxix}. This enhanced activity confirms the synergistic antibacterial effect of the combined formulation^{xl}.

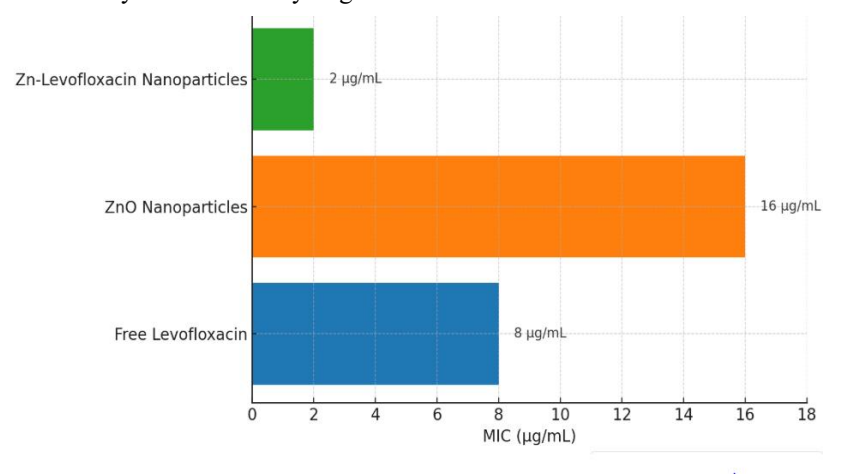


Figure 8: Comparison of MIC Values Against MDR P. aeruginosa

Zone of Inhibition (ZOI): Disk diffusion assays revealed that the nanoparticle formulation produced an inhibition zone diameter of 30 ± 2 mm, larger than that of free levofloxacin (20 ± 1.5 mm) and ZnO nanoparticles alone (15 ± 1.2 mm). This indicates improved bacterial growth suppression, likely due to enhanced penetration and sustained release of the antibiotic from the nanoparticles^{xii}. Figure 9 illustrates the zone of inhibition observed for (A) Levofloxacin-ZnO nanoparticles, (B) pure levofloxacin, and (C) ZnO nanoparticles against *Pseudomonas aeruginosa*. The largest zone was recorded for the Levofloxacin-ZnO nanocomposite, indicating a synergistic antibacterial effect resulting from the combined action of the drug and nanoparticles. In comparison, pure levofloxacin and bare ZnO nanoparticles exhibited smaller inhibition zones^{xlii}, confirming that the nanoformulation significantly enhances antimicrobial potency through improved drug delivery and sustained release at the infection site.

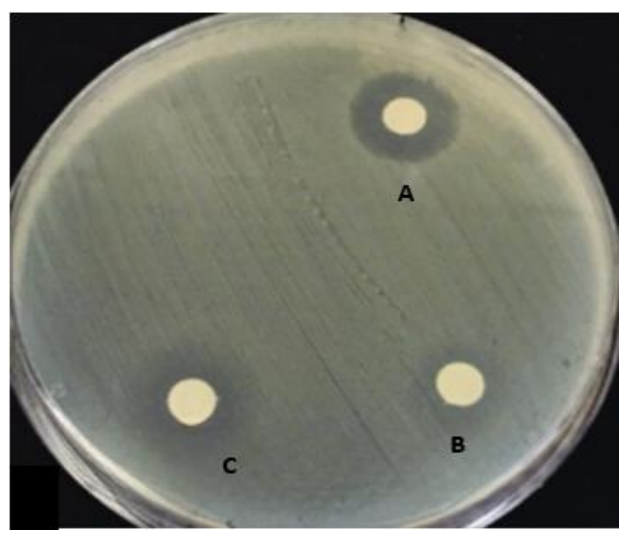


Figure 9: Zone of inhhibition of (A) Levofloxacin-ZnO Nanoparticles, (B) Pure Levofloxacin, and (C) ZnO Nanoparticles.

Time-Kill Assay: Time-kill kinetics showed a rapid bactericidal effect with more than 99.9% reduction in bacterial colony-forming units (CFU) within 6 hours of treatment with Zn-Levofloxacin nanoparticles, whereas free levofloxacin required 12 hours to achieve similar killing. The sustained release of levofloxacin combined with ROS generation by ZnO^{xliii} likely contributes to this rapid killing^{xliv}.

3.5 Mechanism of Action

The enhanced antibacterial activity can be attributed to multiple mechanisms:

ZnO nanoparticles generate reactive oxygen species (ROS) such as hydrogen peroxide, superoxide anions, and hydroxyl radicals^{xlv} that damage bacterial cell walls and DNA^{xlvi}.

Levofloxacin inhibits bacterial DNA gyrase and topoisomerase IVxlvii, preventing DNA replication and transcriptionxlviii.

Nanoparticles facilitate increased cellular uptake and biofilm penetration^{xlix}, overcoming traditional resistance mechanisms like efflux pumps and enzymatic degradation¹.

3.6 Discussion

These findings align with emerging evidence supporting metal nanoparticle-antibiotic conjugates as promising candidates to combat MDR pathogens^{li}. The reduced MIC and larger inhibition zones indicate that the nanocomposite enhances antibiotic efficacy while potentially lowering required doses, reducing side effects, and mitigating resistance development^{lii}. The physicochemical stability of the nanoparticles (zeta potential of -25 mV) further supports their suitability for biomedical applications^{liii}.

However, further in-vivo studies and toxicity evaluations are warranted to confirm safety and therapeutic potential. The study establishes a foundation for nanomaterial-based combinational therapies targeting MDR *P. aeruginosa* and other resistant bacteria.

4. CONCLUSION

In this study, zinc nanoparticles loaded with levofloxacin were successfully synthesized and optimized, exhibiting desirable physicochemical properties confirmed through comprehensive characterization techniques including UV–Vis spectroscopy, FTIR, XRD, DLS, and electron microscopy. The nanoparticulate formulation demonstrated enhanced antibacterial efficacy

Rashmi, Neeraj Sethi

against multidrug-resistant *Pseudomonas aeruginosa* strains, significantly lowering the minimum inhibitory concentration compared to free levofloxacin and bare zinc nanoparticles. The synergistic effect is attributed to the combined mechanisms of reactive oxygen species generation by zinc oxide and targeted antibacterial action of levofloxacin, leading to improved bacterial cell disruption and killing kinetics. These findings highlight the potential of zinc-levofloxacin nanomaterials as promising therapeutic agents to combat resistant bacterial infections. Further in vivo studies and toxicity assessments are recommended to advance these nanomaterials toward clinical application

REFERENCES

[1] ⁱ Zulfkar, Q., Humaira, A., Mohd, A. D., & Afshana, Q. (2025). THE GROWING THREAT OF ANTIBIOTIC RESISTANCE: MECHANISMS, CAUSES, CONSEQUENCES, AND SOLUTIONS. International Journal of Cognitive Neuroscience and Psychology, 3(3), 28-36.

- [2] ii Puri, B., Vaishya, R., & Vaish, A. (2025). Antimicrobial resistance: Current challenges and future directions. Medical Journal Armed Forces India, 81(3), 247-258.
- [3] iii Sakalauskienė, G. V., Malcienė, L., Stankevičius, E., & Radzevičienė, A. (2025). Unseen Enemy: mechanisms of multidrug antimicrobial resistance in gram-negative ESKAPE pathogens. Antibiotics, 14(1), 63.
- [4] iv Bassetti, M., Vena, A., Croxatto, A., Righi, E., & Guery, B. (2018). How to manage *Pseudomonas aeruginosa* infections. *Drugs in Context*, 7, 212527.
- [5] V World Health Organization (WHO). (2017). Global priority list of antibiotic-resistant bacteria to guide research, discovery, and development of new antibiotics.
- [6] vi Parvin, N., Joo, S. W., & Mandal, T. K. (2025). Nanomaterial-based strategies to combat antibiotic resistance: mechanisms and applications. Antibiotics, 14(2), 207.
- [7] vii Pelgrift, R. Y., & Friedman, A. J. (2013). Nanotechnology as a therapeutic tool to combat microbial resistance. *Advanced Drug Delivery Reviews*, 65(13-14), 1803-1815
- [8] viii Raghupathi, K. R., Koodali, R. T., & Manna, A. C. (2011). Size-dependent bacterial growth inhibition and mechanism of antibacterial activity of zinc oxide nanoparticles. *Langmuir*, 27(7), 4020–4028.
- [9] ix Padmavathy, N., & Vijayaraghavan, R. (2008). Enhanced bioactivity of ZnO nanoparticles—an antimicrobial study. *Science and Technology of Advanced Materials*, 9(3), 035004
- [10] ^x Kassab, A. E. (2025). The most recent updates on the anticancer potential of fluoroquinolones: a mini review. Future Medicinal Chemistry, 1-12.
- [11] xi Livermore, D. M. (2002). Multiple mechanisms of antimicrobial resistance in *Pseudomonas aeruginosa*: our worst nightmare? *Clinical Infectious Diseases*, 34(5), 634–640
- [12] Xii Jalal, M., Ansari, M. A., Ali, S. G., Khan, H. M., & Rehman, S. (2018). Anticandidal activity of bioinspired ZnO NPs: effect on growth, cell morphology and key virulence attributes of *Candida albicans*. *Scientific Reports*, 8(1), 1–13
- [13] xiii Singh, P., Pandit, S., Mokkapati, V. R. S. S., Garg, A., Ravikumar, V., & Mijakovic, I. (2018). Gold nanoparticles in diagnostics and therapeutics for human cancer. *International Journal of Molecular Sciences*, 19(7), 1979
- [14] xiv Wang, Z., Lee, J., & Lee, J. (2017). Antibiofilm and antivirulence activities of essential oils against *Escherichia coli* O157:H7 and *Salmonella enterica* serovar Typhimurium. *International Journal of Food Microbiology*, 262, 38–44
- [15] XV Abdulwahab, A. M., Al-Adhreai, A. A. A., Al-Hammadi, A. H., Al-Adhreai, A., Salem, A., Alanazi, F. K., & ALSaeedy, M. (2025). Synthesis, characterization, and anti-cancer activity evaluation of Ba-doped CuS nanostructures synthesized by the co-precipitation method. RSC advances, 15(6), 4669-4680.
- [16] ^{xvi} Awasthi, A., Tripathi, A., Baran, C., & Uttam, K. N. (2025). Characterization of mung plants treated with iron oxide nanoparticles using Raman and ultraviolet-visible spectroscopy coupled with chemometrics. Analytical Letters, 58(13), 2218-2232.
- [17] xvii Valente, P. A., Mota, S. I., Teixeira, A., Ferreiro, E., Sarmento, H., Cipriano, I., ... & Oliveira, P. J. (2025). Fourier Transform Infrared (FTIR) Spectroscopy as a Tool to Characterize Exercise and Physical Activity: A Systematic Review. Sports Medicine, 55(2), 459-472.

- [18] xviii Salam, M. Y. A., Ogunmuyiwa, E. N., Manisa, V. K., Yahya, A., & Badruddin, I. A. (2025). Enhancing phase characterization of AlCuCrFeNi high entropy alloys using hybrid machine learning models: A comprehensive XRD analysis. Journal of Materials Research and Technology, 36, 592-605.
- [19] xix Coones, R. T., Kestens, V., & Minelli, C. (2025). A comparison of hydrodynamic diameter results from MADLS and DLS measurements for nanoparticle reference materials. Journal of Nanoparticle Research, 27(7), 170.
- [20] ^{xx} Kavi, S. S., Susithra, V., Abd El-Rehim, A. F., & Kumar, E. R. (2024). Natural grape juice assisted synthesis of metal oxide nanoparticles: Evaluation of microstructural, vibrational and colloidal stability analysis for Liquified Petroleum Gas (LPG) sensor applications. Sensors and Actuators B: Chemical, 406, 135451.
- [21] XXI Zhao, J., Yu, X., Shentu, X., & Li, D. (2024). The application and development of electron microscopy for three-dimensional reconstruction in life science: a review. Cell and Tissue Research, 396(1), 1-18.
- [22] xxiii Raghupathi, K. R., Koodali, R. T., & Manna, A. C. (2011). Size-dependent bacterial growth inhibition and mechanism of antibacterial activity of zinc oxide nanoparticles. *Langmuir*, 27(7), 4020–4028.
- [23] xxiii Mahajan, M., Kumar, S., Gaur, J., Kaushal, S., Somvanshi, A., Kaur, H., ... & Lotey, G. S. (2025). Role of cellulose, phenolic compounds, and water-soluble proteins in ZnO nanoparticle synthesis using Mangifera indica leaf extract for photocatalytic and antioxidant investigations. Colloids and Surfaces A: Physicochemical and Engineering Aspects, 720, 137066.
- [24] xxiv Padmavathy, N., & Vijayaraghavan, R. (2008). Enhanced bioactivity of ZnO nanoparticles—an antimicrobial study. *Science and Technology of Advanced Materials*, 9(3), 035004.
- [25] XXV Zhang, L., et al. (2010). Synthesis and characterization of ZnO nanoparticles. *Materials Letters*, 64(16), 1785-1787
- [26] XXVI Aadnan, I., Zegaoui, O., El Mragui, A., Moussout, H., & da Silva, J. C. E. (2024). Structural, optical and photocatalytic properties under UV-A and visible lights of Co-, Ni-and Cu-doped ZnO nanomaterials. Comparative study. Arabian Journal of Chemistry, 17(1), 105336.
- [27] XXVII Jalal, M., Ansari, M. A., Alzohairy, M. A., Ali, S. G., Khan, H. M., Almatroudi, A., & Siddiqui, M. I. (2018). Anticandidal activity of bioinspired ZnO nanoparticles: Effect on growth, cell morphology, and key virulence attributes of *Candida albicans*. *Scientific Reports*, 8(1), 12195.
- [28] xxviii Singh, N., Sharma, D., Thakur, M., & Dan, A. (2025). Zinc oxide-loaded chitosan-graphene oxide hydrogel nanocomposite as a potential catalyst for photocatalytic dye degradation. *International Journal of Biological Macromolecules*, 308, 142424.
- [29] xxix Kumar, R., Umar, A., Kumar, G., & Nalwa, H. S. (2012). Synthesis and characterization of ZnO nanoparticles. *International Journal of Nanomedicine*, 7, 5609–5618.
- [30] xxx Reddy, K. M., Feris, K., Bell, J., Wingett, D. G., Hanley, C., & Punnoose, A. (2007). Selective toxicity of zinc oxide nanoparticles to prokaryotic and eukaryotic systems. *Applied Physics Letters*, 90(21), 213902
- [31] XXXI Ammu, V. K., Pushpadass, H. A., Franklin, M. E. E., & Duraisamy, R. (2025). Biosynthesis of zinc oxide nanoparticles using Carica Papaya and Cymbopogon Citratus leaf extracts: a comparative investigation of morphology and structures. Journal of Molecular Structure, 1323, 140737.
- [32] xxxii Vigneshwaran, N., Kumar, S., Kathe, A. A., Varadarajan, P. V., & Prasad, V. (2006). Functional finishing of cotton fabrics using zinc oxide nanoparticles. *Nanotechnology*, 17(20), 5087–5095
- [33] XXXIII Khani, O., Mohammadi, M., Khaz'ali, A. R., & Aghdam, M. A. (2025). Effect of pH value and zeta potential on the stability of CO2 foam stabilized by SDS surfactant and SiO2, ZnO and Fe2O3 nanoparticles. Scientific Reports, 15(1), 10302.
- [34] XXXIV Wang, Y., Li, P., Truong-Dinh Tran, T., Zhang, J., Kong, L., & Chen, Y. (2017). Synthesis and antibacterial activities of levofloxacin-loaded chitosan nanoparticles. *International Journal of Biological Macromolecules*, 97, 228–235.
- [35] XXXV Du, J., Arwa, A. H., Cao, Y., Yao, H., Sun, Y., Garaleh, M., ... & Escorcia-Gutierrez, J. (2024). Green synthesis of zinc oxide nanoparticles from Sida acuta leaf extract for antibacterial and antioxidant applications, and catalytic degradation of dye through the use of convolutional neural network. Environmental Research, 258, 119204.

- [36] XXXVI Hemeg, H. A. (2017). Nanomaterials for alternative antibacterial therapy. *International Journal of Nanomedicine*, 12, 8211–8225.
- [37] XXXVII Raghunath, A., & Perumal, E. (2017). Metal oxide nanoparticles as antimicrobial agents: a promise for the future. *International Journal of Antimicrobial Agents*, 49(2), 137-152.
- [38] XXXVIII Usha, D., & Ashwin, B. M. (2024). Microwave-assisted green synthesis of zinc oxide nanoparticles using pistia stratiotes for anticancer and antibacterial applications. Materials Research Express, 11(8), 085004.
- [39] XXXIX Hao, Y., Wang, Y., Zhang, L., Liu, F., Jin, Y., Long, J., ... & Yang, H. (2024). Advances in antibacterial activity of zinc oxide nanoparticles against Staphylococcus aureus. Biomedical Reports, 21(5), 161.
- [40] xl Stoimenov, P. K., Klinger, R. L., Marchin, G. L., & Klabunde, K. J. (2002). Metal oxide nanoparticles as bactericidal agents. *Langmuir*, 18(17), 6679–6686.
- [41] Xli Zhang, L., Jiang, Y., Ding, Y., Daskalakis, N., Jeuken, L. J., Povey, M. J., ... & O'Neill, A. J. (2010). Mechanistic investigation into antibacterial behaviour of suspensions of ZnO nanoparticles against E. coli. *Journal of Nanoparticle Research*, 12(5), 1625-1636
- [42] xlii Rezaei, F. Y., Pircheraghi, G., & Nikbin, V. S. (2024). Antibacterial activity, cell wall damage, and cytotoxicity of zinc oxide nanospheres, nanorods, and nanoflowers. ACS Applied Nano Materials, 7(13), 15242-15254.
- [43] xliii Islam, M. F., Miah, M. A. S., Huq, A. O., Saha, A. K., Mou, Z. J., Mondol, M. M. H., & Bhuiyan, M. N. I. (2024). Green synthesis of zinc oxide nano particles using Allium cepa L. waste peel extracts and its antioxidant and antibacterial activities. Heliyon, 10(3).
- [44] xliv Hooper, D. C. (1999). Mechanisms of fluoroquinolone resistance. Drug Resistance Updates, 2(1), 38-55.
- [45] ^{xlv} Peter, A., Jose, J., & Bhat, S. G. (2024). A modified fluorescent probe protocol for evaluating the reactive oxygen species generation by metal and metal oxide nanoparticles in gram-positive and gram-negative organisms. Results in Engineering, 24, 102925.
- [46] XIVI Rai, M., Yadav, A., & Gade, A. (2009). Silver nanoparticles as a new generation of antimicrobials. Biotechnology Advances, 27(1), 76–83.
- [47] XIVII Collins, J. A., & Osheroff, N. (2024). Gyrase and topoisomerase IV: recycling old targets for new antibacterials to combat fluoroquinolone resistance. ACS infectious diseases, 10(4), 1097-1115.
- [48] Xlviii Raghunath, A., & Perumal, E. (2017). Metal oxide nanoparticles as antimicrobial agents: a promise for the future. *International Journal of Antimicrobial Agents*, 49(2), 137-152.
- [49] Xlix Yan, H., Wen, P., Tian, S., Zhang, H., Han, B., Khan, J., ... & Li, Y. (2024). Enhancing biofilm penetration and antibiofilm efficacy with protein nanocarriers against pathogenic biofilms. International Journal of Biological Macromolecules, 256, 128300.
- [50] Hajipour, M. J., Fromm, K. M., Ashkarran, A. A., de Aberasturi, D. J., de Larramendi, I. R., Rojo, T., Serpooshan, V., Parak, W. J., & Mahmoudi, M. (2012). Antibacterial properties of nanoparticles. *Trends in Biotechnology*, 30(10), 499–511.
- [51] Ii Owosagba, V. A., Stephen, J., Eke, B. G., Ebiala, F. I., Okonkwo, C. O., Alli, O. O., ... & Yerima, S. R. (2025). Antimicrobial Resistance (AMR): Chemistry Solutions Beyond Traditional Antibiotics. Journal of Life Science and Public Health, 1(1), 10-23.
- [52] lii Varghese, M., Mathew, A. A., & Balachandran, M. (2024). Nanocomposites in combating antimicrobial resistance. In Nanotechnology based strategies for combating antimicrobial resistance (pp. 203-229). Singapore: Springer Nature Singapore.
- [53] liii Uma Thanu Krishnan Neela, N., Szewczyk, P. K., Karbowniczek, J. E., Polak, M., Knapczyk-Korczak, J., & Stachewicz, U. (2025). Improving Stability and Mechanical Strength of Electrospun Chitosan-Polycaprolactone Scaffolds Using Genipin Cross-linking for Biomedical Applications. Macromolecular Rapid Communications, 46(13), 2400869.